Homogenized models of electrically coupled excitable tissues

Pranay Goel
Indian Institute of Science Education and Research Pune

COMSOL Conference
Bangalore 4-5 November, 2011

Acknowledgements

- Avner Friedman, Ohio State U.
- James Sneyd, U. of Auckland
- Arthur Sherman, US National Institutes of Health

- (The nice folk at) COMSOL!

Excitability

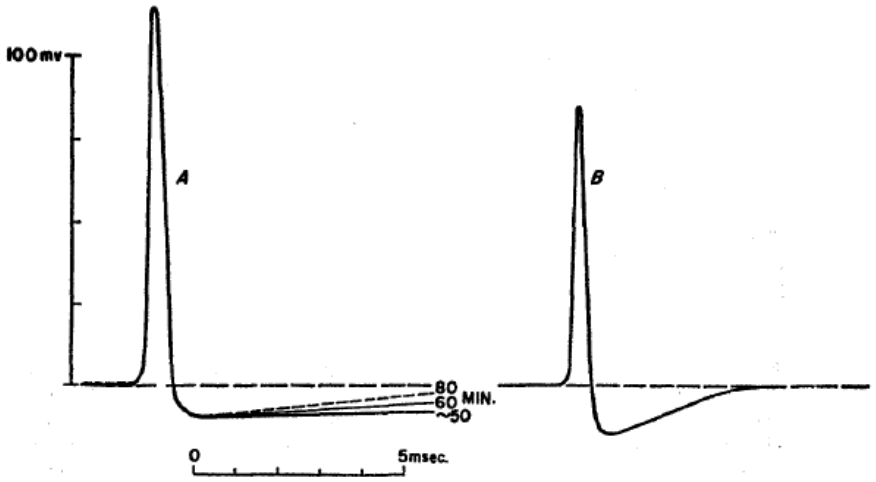

FIGURE 2. A, squid axon membrane action potentials *in vivo*. The rate of recovery from the undershoot increased as shown with time after the initial cutting of the mantle. Temperature 20°C. B, action potential in a mantle preparation showing a somewhat larger and much more rapid recovery from the undershoot. This record was taken during the midsummer slump and gave a typically lower peak action potential.

J. W. Moore and K. S. Cole, *Resting and action potentials of the squid giant axon in vivo*, JGP (1960).

- The Nobel Prize in Physiology or Medicine 1963 was awarded jointly to Sir John Carew Eccles, Alan Lloyd Hodgkin and Andrew Fielding Huxley *"for their discoveries concerning the ionic mechanisms involved in excitation and inhibition in the peripheral and central portions of the nerve cell membrane"*.

Pancreatic insulin secretion

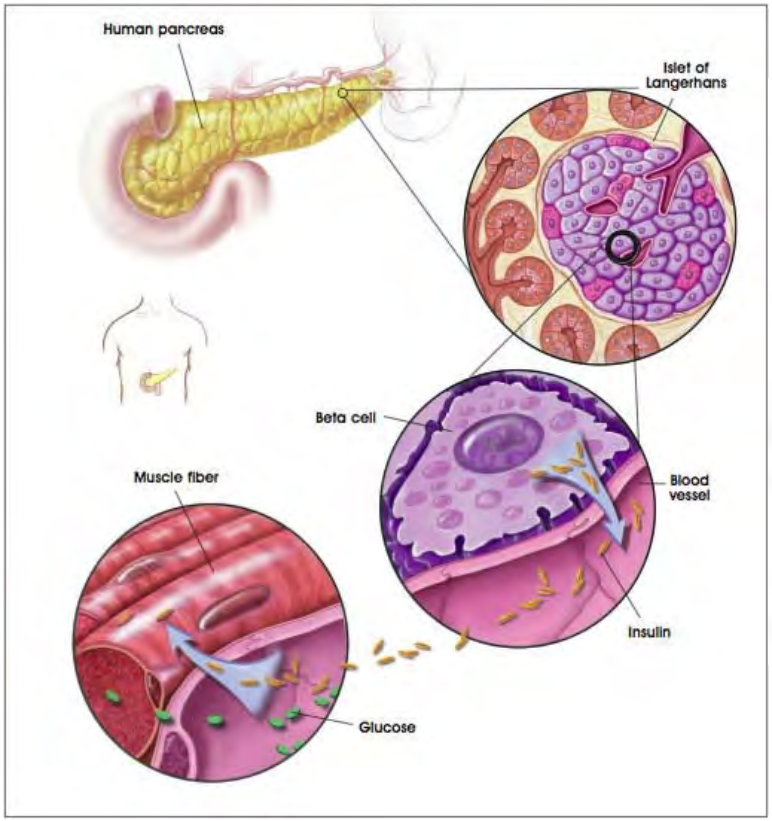

Terese Winslow, Lydia Kibiuk
http://stemcells.nih.gov

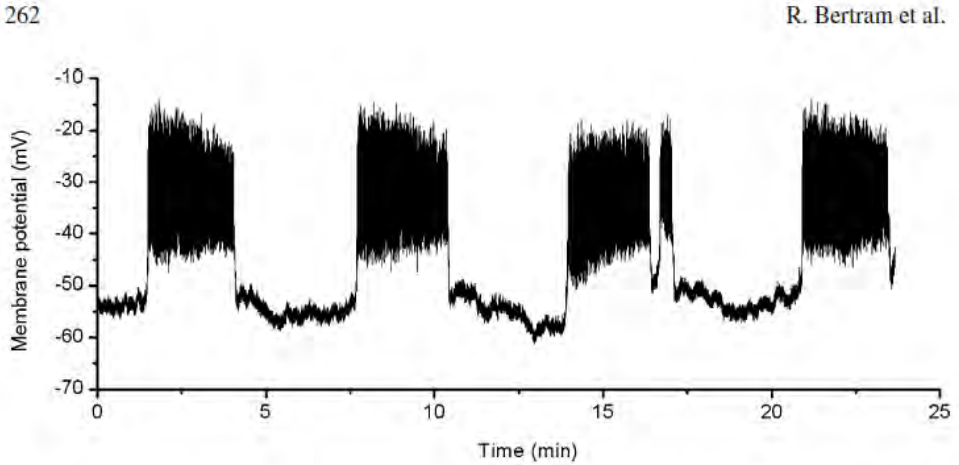

Fig. 12.1 Slow electrical bursting recorded from a mouse islet. Provided by J. Ren and L.S. Satin

Gap junctions

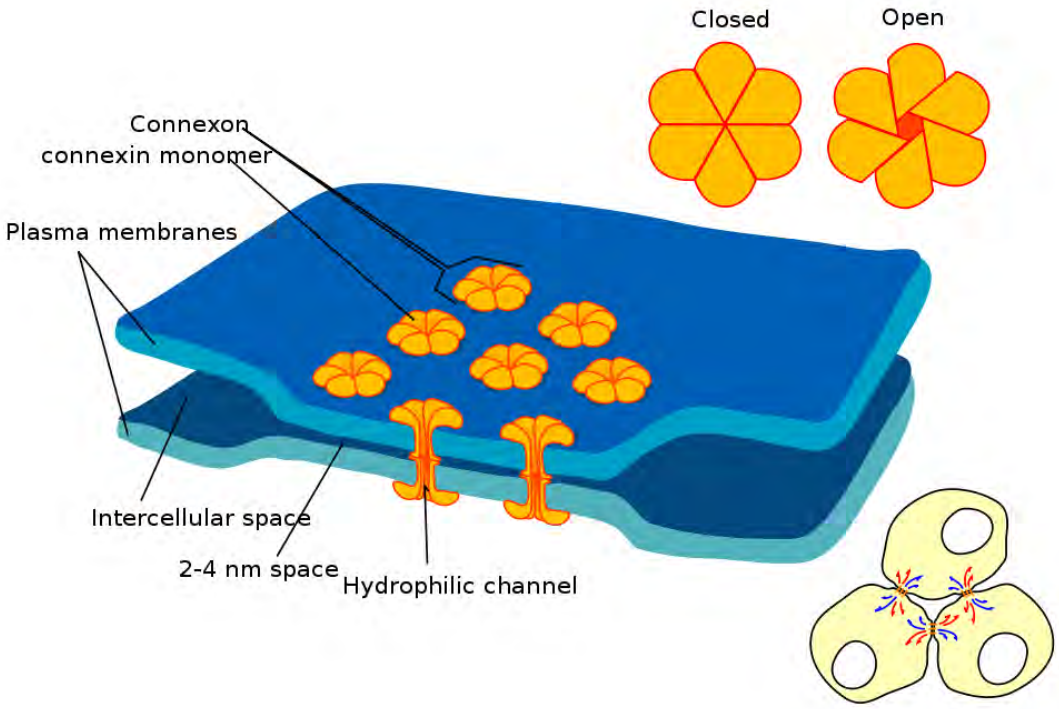

Mariana Ruiz, Wikimedia Commons

- Gap junctions facilitate a direct electrical and chemical connectivity

Homogenized models of islets

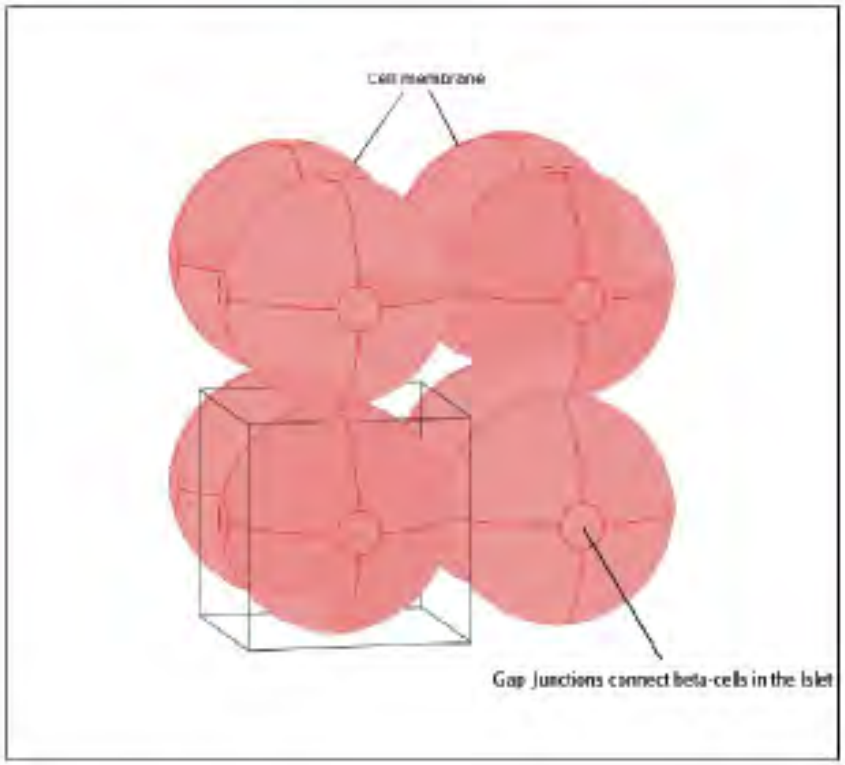

FIG. 1. *The periodic geometry of beta-cells connected through gap junctions.*

Homogenization: the microscopic problem

(2.1a)
$$\nabla \cdot (\sigma^{i,e}_\varepsilon \nabla \phi^\varepsilon_{i,e}) = 0, \quad x \in \Omega^\varepsilon_{i,e}, \qquad \text{(quasi-static conduction)}$$

(2.1b)
$$\frac{\partial c^\varepsilon_e}{\partial t} = \nabla \cdot (D^e_\varepsilon \nabla c^\varepsilon_e), \quad x \in \Omega^\varepsilon_e, \qquad \text{(extracellular calcium diffusion)}$$

(2.1c)
$$\frac{\partial c^\varepsilon_i}{\partial t} = \nabla \cdot (D^i_\varepsilon \nabla c^\varepsilon_i) + j_{ER}(c^\varepsilon_i, s^\varepsilon) + k_{c-} b^\varepsilon_c - k_{c+} c^\varepsilon_i (B_c - b^\varepsilon_c), \quad x \in \Omega^\varepsilon_i, \qquad \text{(cytosolic calcium diffusion)}$$

(2.1d)
$$\frac{\partial b^\varepsilon_c}{\partial t} = \nabla \cdot (M^c_\varepsilon \nabla b^\varepsilon_c) - k_{c-} b^\varepsilon_c + k_{c+} c^\varepsilon_i (B_c - b^\varepsilon_c), \quad x \in \Omega^\varepsilon_i, \qquad \text{(cytosolic buffering)}$$

(2.1e)
$$\frac{\partial s^\varepsilon}{\partial t} = \nabla \cdot (D^s_\varepsilon \nabla s^\varepsilon) - j_{ER}(c^\varepsilon_i, s^\varepsilon) + k_{s-} b^\varepsilon_s - k_{s+} s^\varepsilon (B_s - b^\varepsilon_s), \quad x \in \Omega^\varepsilon_i, \qquad \text{(ER calcium)}$$

(2.1f)
$$\frac{\partial b^\varepsilon_s}{\partial t} = \nabla \cdot (M^s_\varepsilon \nabla b^\varepsilon_s) - k_{s-} b^\varepsilon_s + k_{s+} s^\varepsilon (B_s - b^\varepsilon_s), \quad x \in \Omega^\varepsilon_i, \qquad \text{(ER buffering)}$$

(2.1g)
$$v = \phi_i - \phi_e,$$

where $\sigma^{i,e}_\varepsilon = \sigma^{i,e}(\frac{x}{\varepsilon})$ are the intracellular and extracellular conductivity matrices and $D^{i,e,s}_\varepsilon = D^{i,e,s}(\frac{x}{\varepsilon})$, $M^{c,s}_\varepsilon = M^{c,s}(\frac{x}{\varepsilon})$ are the calcium and buffer diffusion coefficients.

The boundary conditions on the membrane Γ^ε, which separates Ω^ε_i from Ω^ε_e, are given by (also see appendix 8.1)

(2.2a) $$-\sigma^i_\varepsilon \nabla \phi^\varepsilon_i \cdot \nu^\varepsilon_i = \varepsilon \left(c_m \frac{\partial v^\varepsilon}{\partial t} + i_{ion}(v^\varepsilon, n^\varepsilon, c^\varepsilon_i, c^\varepsilon_e) \right),$$

(2.2b) $$\sigma^e_\varepsilon \nabla \phi^\varepsilon_e \cdot \nu^\varepsilon_e = \varepsilon \left(c_m \frac{\partial v^\varepsilon}{\partial t} + i_{ion}(v^\varepsilon, n^\varepsilon, c^\varepsilon_i, c^\varepsilon_e) \right),$$

(2.2c) $$D^e_\varepsilon \nabla c^\varepsilon_e \cdot \nu^\varepsilon_e = \varepsilon \left(\alpha\, i_{Ca}(v^\varepsilon, n^\varepsilon, c^\varepsilon_i, c^\varepsilon_e) + j_{PMCA}(c^\varepsilon_i, c^\varepsilon_e) \right),$$

(2.2d) $$-D^i_\varepsilon \nabla c^\varepsilon_i \cdot \nu^\varepsilon_i = \varepsilon \left(\alpha\, i_{Ca}(v^\varepsilon, n^\varepsilon, c^\varepsilon_i, c^\varepsilon_e) + j_{PMCA}(c^\varepsilon_i, c^\varepsilon_e) \right),$$

(2.2e) $$M^c_\varepsilon \nabla b^\varepsilon_c \cdot \nu^\varepsilon_i = 0 \quad \text{on } \Gamma^\varepsilon,$$

(2.2f) $$D^s_\varepsilon \nabla s^\varepsilon \cdot \nu^\varepsilon_i = 0 \quad \text{on } \Gamma^\varepsilon, \qquad D^s_\varepsilon \nabla s^\varepsilon \cdot \nu^\varepsilon_g = 0 \quad \text{on } \Gamma^\varepsilon_g,$$

(2.2g) $$M^s_\varepsilon \nabla b^\varepsilon_s \cdot \nu^\varepsilon_i = 0 \quad \text{on } \Gamma^\varepsilon, \qquad M^s_\varepsilon \nabla b^\varepsilon_s \cdot \nu^\varepsilon_g = 0 \quad \text{on } \Gamma^\varepsilon_g,$$

(2.2h) $$\frac{\partial n^\varepsilon}{\partial t} = g(v^\varepsilon, n^\varepsilon, c^\varepsilon_i, c^\varepsilon_e),$$

where n^ε represents gating variables corresponding to ion channels and ν^ε_i and ν^ε_e denote the unit exterior normals to the boundary of Ω^ε_i and Ω^ε_e, respectively, satisfying $\nu^\varepsilon_i = -\nu^\varepsilon_e$ on Γ^ε. Here ν_g is the unit exterior normal on the gap junction pore Γ^ε_g (Figure 2), c_m is the membrane capacitance per unit area, and i_{ion} is the ionic current per unit area. We have assumed that ER calcium, and the buffers it interacts with, are restricted to each beta-cell. On the other hand, cytosolic calcium and buffers are both assumed to diffuse through gap junctions. Below we will explicitly consider cases when this assumption is weakened. Throughout the paper we will assume that intracellular space is continuous with respect to electrical potential, ϕ^ε_i.

Goel, Sherman and Friedman, *The islet tridomain equations*, SIAM MMS (2009).

Homogenization: the microscopic problem

$\phi^\varepsilon_{i,e} = \phi(x,\xi,t), \quad c^\varepsilon_{i,e} = c_{i,e}(x,\xi,t), \quad b^\varepsilon_c = b_c(x,\xi,t), \quad s^\varepsilon = s(x,\xi,t), \quad b^\varepsilon_s = b_s(x,\xi,t)$

with $\xi = x/\varepsilon$. The formal asymptotic expansions for ϕ^ε_i and ϕ^ε_e are of the form

$$\begin{aligned}
\phi^\varepsilon_{i,e} &= \phi^0_{i,e}(x,\xi,t) + \varepsilon\phi^1_{i,e}(x,\xi,t) + \varepsilon^2\phi^2_{i,e}(x,\xi,t) + \cdots, \\
c^\varepsilon_{i,e} &= c^0_{i,e}(x,\xi,t) + \varepsilon c^1_{i,e}(x,\xi,t) + \varepsilon^2 c^2_{i,e}(x,\xi,t) + \cdots, \\
b^\varepsilon_c &= b^0_c(x,\xi,t) + \varepsilon b^1_c(x,\xi,t) + \varepsilon^2 b^2_c(x,\xi,t) + \cdots, \\
s^\varepsilon &= s^0(x,\xi,t) + \varepsilon s^1(x,\xi,t) + \varepsilon^2 s^2(x,\xi,t) + \cdots, \\
b^\varepsilon_s &= b^0_s(x,\xi,t) + \varepsilon b^1_s(x,\xi,t) + \varepsilon^2 b^2_s(x,\xi,t) + \cdots,
\end{aligned}$$

where

$$\phi^k_{i,e}(\cdot,\xi),\ c^k_{i,e}(\cdot,\xi),\ b^k_c(\cdot,\xi),\ s^k(\cdot,\xi), \text{ and } b^k_s(\cdot,\xi) \text{ are 1-periodic in } \xi.$$

Setting

$$\nabla \equiv \frac{\mathrm{d}}{\mathrm{d}x} = \nabla_x + \varepsilon^{-1}\nabla_\xi,$$

it follows that the operator $\nabla\cdot(\mathcal{A}_\varepsilon\nabla)$ acts on a function of (x,ξ) with $\xi = \frac{x}{\varepsilon}$ as follows:

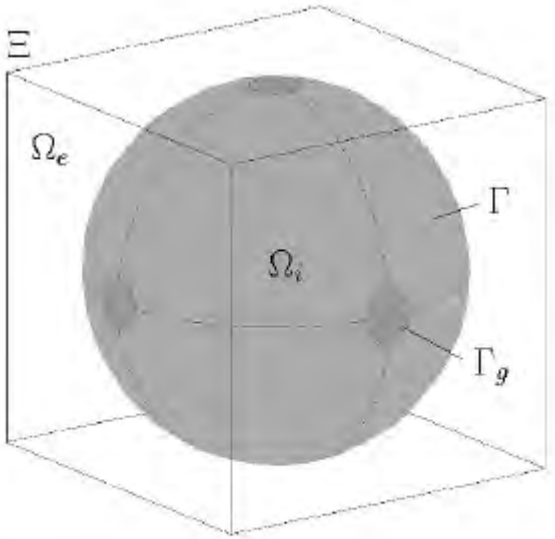

FIG. 2. *The periodic unit cell.*

Homogenization: the macroscopic equations

3. A reduction of the macroscopic equations. In section 2 it was shown the macroscopic (average) equations[2] for the islet are

$$v = \phi_i - \phi_e, \tag{3.1a}$$

$$C_m \frac{\partial v}{\partial t} = \nabla \cdot (\tilde{\sigma}^i \nabla \phi_i) - I_{ion}(v, n, c_i, c_e), \tag{3.1b}$$

$$C_m \frac{\partial v}{\partial t} = -\nabla \cdot (\tilde{\sigma}^e \nabla \phi_e) - I_{ion}(v, n, c_i, c_e), \tag{3.1c}$$

$$\gamma_e \frac{\partial c_e}{\partial t} = \nabla \cdot (\tilde{D}^e \nabla c_e) + \Lambda \left[\alpha \, i_{Ca}(v, n, c_i, c_e) + j_{PMCA}(c_i, c_e) \right], \tag{3.1d}$$

$$\gamma_i \frac{\partial c_i}{\partial t} = \nabla_x \cdot (\tilde{D}^i \nabla_x c_i) - \Lambda \left(\alpha \, i_{Ca}(v, n, c_i, c_e) + j_{PMCA}(c_i, c_e) \right)$$

$$+ \gamma_i \left(j_{ER}(c_i, s) + k_{c-} b_c - k_{c+} c_i (B_c - b_c) \right), \tag{3.1e}$$

$$\gamma_i \frac{\partial b_c}{\partial t} = \nabla_x \cdot (\tilde{M}^c \nabla_x b_c) - \gamma_i \left(k_{c-} b_c - k_{c+} c_i (B_c - b_c) \right), \tag{3.1f}$$

$$\frac{\partial s}{\partial t} = \left(-j_{ER}(c_i, s) + k_{s-} b_s - k_{s+} s (B_s - b_s) \right), \tag{3.1g}$$

$$\frac{\partial b_s}{\partial t} = -\left(k_{s-} b_s - k_{s+} s (B_s - b_s) \right), \tag{3.1h}$$

$$\frac{\partial n^\varepsilon}{\partial t} = g(v^\varepsilon, n^\varepsilon, c_i^\varepsilon, c_e^\varepsilon), \tag{3.1i}$$

where $C_m = \Lambda c_m$ and $I = \Lambda i$ are the total membrane capacitance and currents, respectively. As a special case of these equations we can assume isotropy of the conductivity—a good approximation, since the beta-cells are roughly spherical—to be $\tilde{\sigma}^i = \lambda \tilde{\sigma}^e$. Then (3.1b) and (3.1c) can be reduced to

$$C_m \frac{\partial v}{\partial t} = \nabla \cdot \left(\frac{\lambda}{1+\lambda} \tilde{\sigma}^i \nabla v \right) - I_{ion}(v, n, c_i, c_e). \tag{3.2}$$

Equations (3.1d), (3.1e), (3.1f), (3.1g), (3.1h), (3.1i), and (3.2) constitute the reduced islet bidomain equations.

The cell-problem for syncytial coupling

$$-\nabla \cdot (A(\nabla_y \chi + I)) = 0 \tag{1.1}$$

on the intracellular domain, Ω_i, in the unit cube Y, for a Y-periodic function, χ, together with the boundary condition

$$-A(\nabla_y \chi + I) \cdot \eta = 0 \tag{1.2}$$

on the membrane boundary Γ_m, with η the normal outward to the cell. The homogenized conductivity tensor is computed as

$$\tilde{A}_{syncytial} = \int_{\Omega_i} A(\nabla_y \chi + I). \tag{1.3}$$

- The same calculation is useful for computing both, the effective diffusion coefficient (to, say intracellular calcium) as well as the effective electrical conductivity.

Syncytial coupling in the islet: cell problem solutions

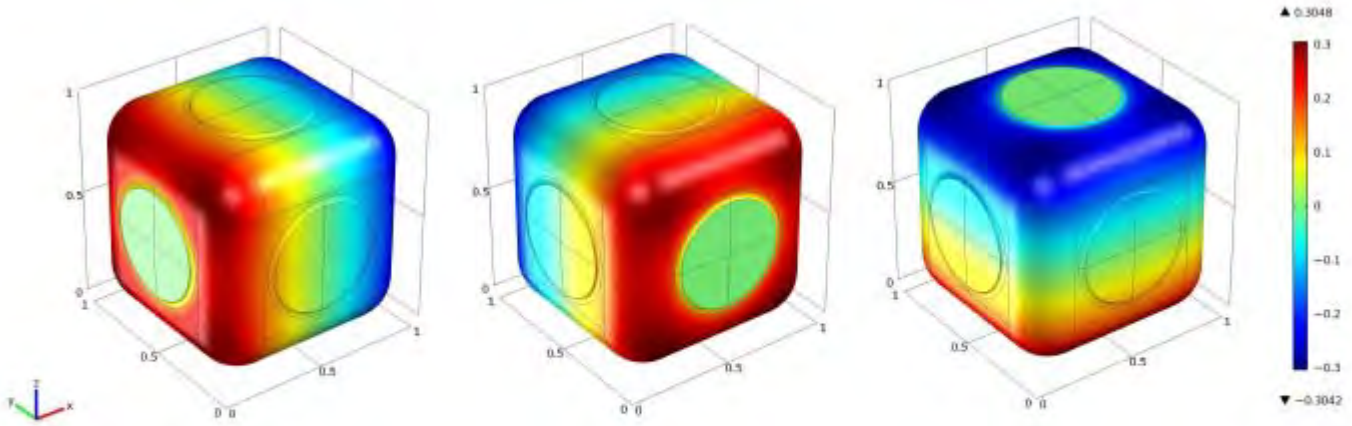

FIG. 4.1. *The scalar fields, χ_1, χ_2, χ_3, that are the solutions to the cell problem for a cuboidal cell assuming syncytial coupling. Notice that the field is 1-periodic, but otherwise arbitrary up to a constant; the midpoint of the Y-Z face was therefore constrained to be at $\chi_1 = \chi_2 = \chi_3 = 0$.*

in Section 3.1 cast suitably in three dimensions. The homogenized diffusion coefficient is computed to be 0.516; the volume of this cuboid is 0.866, so the effective diffusion coefficient is 0.595.

“Doughball” coupling in the islet: an alternative model

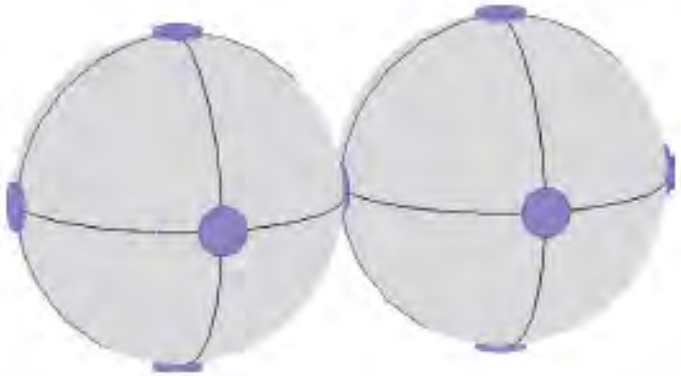

FIG. 13. *A simple model of gap junctions that can account for a possibly marked difference between the conductivities of the junctional plate and the cytoplasm: the junctional plate is modeled as a* thin *circular ohmic conductor sandwiched between neighboring cells.*

The cell-problem for doughball coupling

In the case of the dough ball model, a coupled pair of cell problems need to be solved instead:

$$-\nabla \cdot (A(\nabla_y \chi + I)) = 0, \tag{1.4}$$

$$-\nabla \cdot (A(\nabla_y \xi + I)) = 0, \tag{1.5}$$

for Y-periodic functions χ and ξ each defined on alternate cells, $\Omega_{1,2}$ in Y, with boundary conditions on the gap junction (now a boundary between cells) Γ_g:

$$-A(\nabla_y \chi + I) \cdot \eta = A(\nabla_y \xi + I) \cdot \eta, \tag{1.6}$$

$$-A(\nabla_y \chi + I) \cdot \eta = g(\chi - \xi), \tag{1.7}$$

and

$$-A(\nabla_y \chi + I) \cdot \eta = 0, \tag{1.8}$$

$$-A(\nabla_y \xi + I) \cdot \eta = 0, \tag{1.9}$$

on the membrane apart of the gap junctions, $\Gamma \backslash \Gamma_g$. The homogenized conductivity tensor is now computed as

$$\tilde{A}_{dough\ ball} = \int_{\Omega_1} A(\nabla_y \chi + I) + \int_{\Omega_2} A(\nabla_y \xi + I). \tag{1.10}$$

Doughball cell problems in the islet

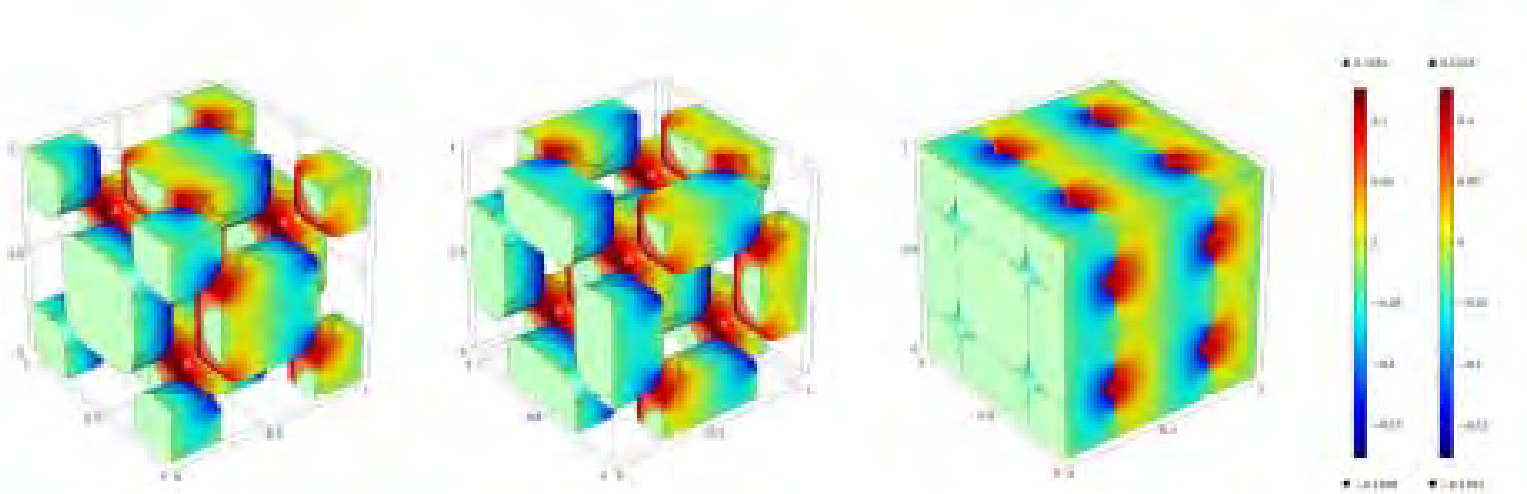

FIG. 4.3. *The scalar fields, χ_1 and ξ_1, corresponding to the cell problem solved for $g_{gap} = 1e4$. The first two panels show χ_1 and ξ_1 separately on their respective domains while the third panel shows them together in the cube for direct comparison. As above, the point $(0,0,0)$ (the lowermost point in the cube in these figures) was constrained to $\chi_1 = \chi_2 = \chi_3 = 0$ and each of the fields is 1-periodic. Also compare to Figure 4.2 above.*

Homogenized coefficients as a function of gap-junctional permeability

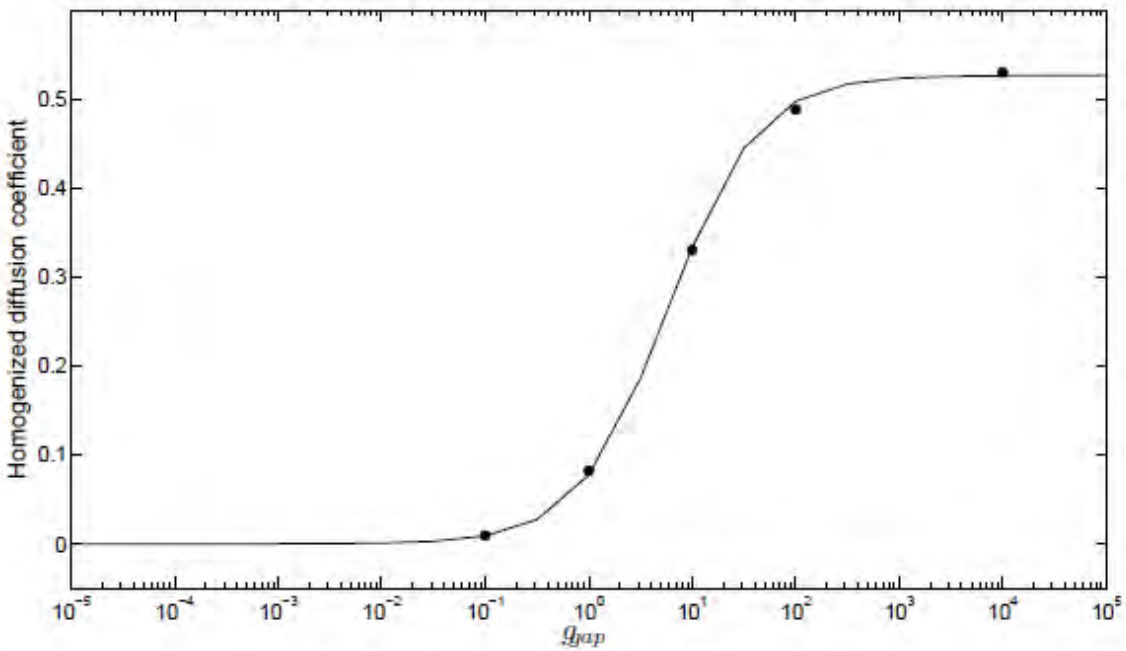

FIG. 4.4. *The homogenized diffusion coefficient for a realistic 3D cellular geometry (see above) computed numerically for several values of* g_{gap}*(dots), and a best-fit sigmoidal curve,* $g_{gap}/(1.9\ g_{gap} + 20)$.

Low conductivity can explain wave propagation failure

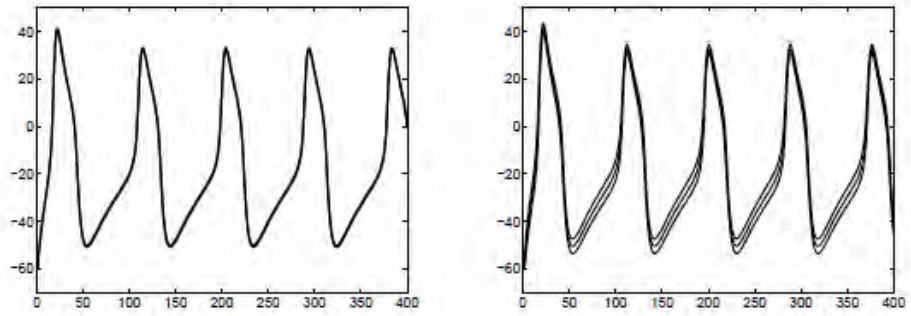

(a) $\sigma = 1 \times 10^5$.

(b) $\sigma = 1 \times 10^3$.

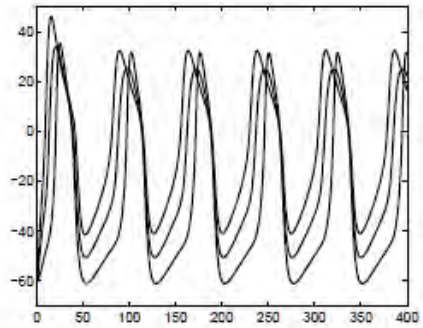

(c) $\sigma = 1 \times 10^2$.

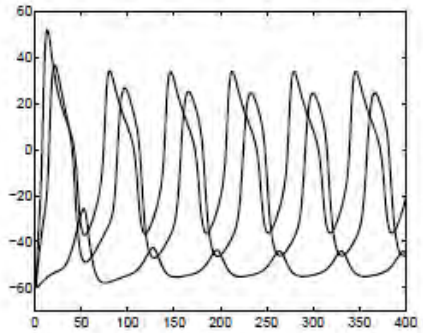

(d) $\sigma = 10$.

FIG. 4.1. *Travelling wave solutions in the islet for varying values of σ. The plots are displayed at three points: the two endpoints, and at $x = 5$.*

Partially propagating waves at very low conductivity

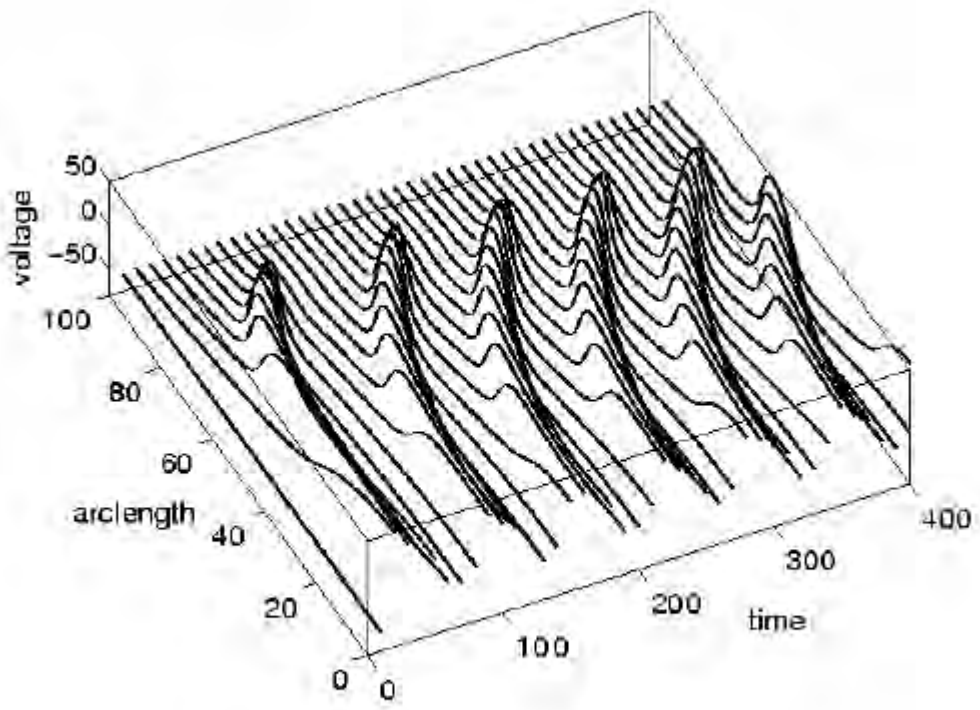

Conclusions

- It seems that both synchrony as well as wave propagation failure in islets can be explained
- if the conductivity is modulated over two orders of magnitude.
- Using a reasonable estimate of large/small sizes of gap junctional plaques, a syncytial model seems to admit a conductivity change of only about ½.
- The doughball model (parameterized by g_gap), on the other hand, allows a much wider span of conductivities in the tissue.
- The doughball model might be a more effective model of gap junctional connectivity in islets.

Open questions

- A fuller, systematic comparison of syncytial and doughball models
- A derivation of g_gap from an underlying microscopic geometry
- Embedding the gap junctional models in more realistic islet dynamics